Arabian Journal of Chemistry (2021) 14, 103449

King Saud University

Arabian Journal of Chemistry

www.ksu.edu.sa
www.sciencedirect.com

ORIGINAL ARTICLE

2-methylindole analogs as cholinesterases and glutathione S-transferase inhibitors: Synthesis, biological evaluation, molecular docking, and pharmacokinetic studies

Adnan Cetin [a,*], **Ercan Bursal** [a], **Fikret Türkan** [b]

[a] *Faculty of Health Sciences, University of Mus Alparslan, Mus 49250, Turkey*
[b] *Health Services Vocational School, Igdir University, 76000 Igdir, Turkey*

Received 29 July 2021; accepted 15 September 2021
Available online 22 September 2021

KEYWORDS

Acetylcholinesterase;
Computational studies;
Drug design;
Enzyme inhibition;
Molecular docking

Abstract In this study, we aimed to (i) synthesize new 2-methylindole analogs containing various amino structures, pyrrolidine, piperidine, morpholine, and substituted phenyl groups through structural and molecular modifications, (ii) evaluate the pharmaceutical potential of 2-methylindole analogs via assessing enzyme inhibitory activity against glutathione S-transferase (GST), acetylcholinesterase (AChE), and butyrylcholinesterase (BChE), (iii) predict ADMET and pharmacokinetic properties of the synthesized 2-methylindole analogs, (iv) reveal the possible interactions between the synthesized 2-methylindole analogs with GST, AChE, and BChE enzymes using several molecular docking software. *In vitro* enzyme inhibition assays showed that the synthesized indole analogs exhibited moderate to good inhibitory activities against GST, AChE, and BChE enzymes. Briefly, the inhibitory activities of the analogs **4b** and **4i** against AChE, **4a** and **4b** against BChE, and analogs **1** and **4i** against GST were detected to be higher or close to the standard inhibitor compounds. The analog **4b** was detected to have the best inhibitory activity against both AChE and BChE enzymes with the lowest IC_{50} values as 0.648 μM for AChE and 0.745 μM for BChE. The analyses of enzyme inhibition relationship with the synthesized analogs could help to design new analogs for the inhibitors of cholinergic and glutathione pathways based on the indole derivatives.

1. Introduction

Syntetic organic compounds particularly nitrogen-containing heterocyclic molecules, such as pyrazole, imidazole, and indole derivatives have been accepted to be the important raw materials for the pharmaceutical industry due to their biological activity properties (Zhang et al., 2015, Singh et al., 2021a,b).

* Corresponding author.
E-mail address: adnankimya@gmail.com (A. Cetin).
Peer review under responsibility of King Saud University.

Production and hosting by Elsevier

https://doi.org/10.1016/j.arabjc.2021.103449
1878-5352

Several substituted indole analogs serve as potential pharmacophores that exert multiple pharmacological properties (Dvořák et al., 2021). Indole scaffolds which are bicyclic aromatic heterocyclic compounds have drawn attention in drug discovery due to their broad-spectrum biological activities, such as anti neurodegenerative (Goyal and Kaur, 2018), antidepressant (Hamid et al.,2017), antihyperglycemic (Solangi et al., 2020), anti-inflammatory (da Silva Guerra et al., 2011), and antimicrobial (Gurkok et al., 2009) activities. Furthermore, many indole analogs were successfully commercialized in the pharmacology, medicine, and biotechnology fields. The structures of several commercial drugs that developed from indole scaffolds are shown in Fig. 1. Some of the indole-containing drugs, such as panobistat (anti-leukemic drug), oxypertine (antipsychotic), roxindole (schizophrenia) (Cheng et al., 2019, Durell and Pollin, 1963, Kasper et al., 1992), delavirdine and umifenovir (antiviral drugs) (Demeter et al., 2000, Blaising et al., 2014), sumatriptan (anti-migraine headaches) (Dechant and Clissold, 1992), indolmycin (antibiotic) (Harnden et al., 1978), pindolol (beta blocker) (Roberts et al., 1987), golotimod (STAT3 inhibitor) (Geiger et al., 2016) and indapamide (anti-hypertension) (Chaffman et al., 1984) have been used in pharmaceutical industry. In addition, some of the indole molecules were reported as effective therapeutic agents and potentially utilized in the rational drug design (Dinnell et al., 2001).

The inhibitions of enzymes in some metabolic pathways are the key attributes for the treatments of some health problems (Grochowski et al., 2017). For instance, acetylcholinesterase inhibition has been thought to play a major role in the pathogenesis of Alzheimer's disease (AD) (Singh et al., 2021a,b). AChE and BChE enzymes are involved in a large variety of possible brain disease processes including neurological and immune functions (Makhaeva et al., 2015). The cholinesterase enzymes are highly relevant targets for drug therapy, thus many cholinesterase inhibitors have been used as drugs for the treatment of Alzheimer's disease and some neuromuscular disorders (Mughal et al., 2020., Mumtaz et al., 2019). The FDA (U.S. Food and Drug Administration) has approved approximately more than 300 drugs as AChE and BChE inhibitors (GN et al., 2020). Also, the GST enzyme emerged as a promising therapeutic target and plays critical roles against oxidative stress, tumor occurrence, detoxification mechanisms, and drug resistance (Morgan et al., 1996., Schultz et al., 1997).

To explore new chemical structures for the ligand prediction of AChE, BChE, and GST enzymes appears to be an inspiring goal of scientific attention in recent years (Aras et al., 2021, Turkan et al., 2018, Turkan et al., 2019). Indeed, various small molecular scaffolds, such as indoles, pyrazoles, thiophenes, and pyridazines were investigated for their functions in the ligand-based enzyme experiments (Erlanson et al., 2020). It is important to note the difference between molecular motifs and simply common in drug discovery, and organic small molecules are generally rigid aromatic structures that well-defined binding pockets in the AChE, BChE, and GST target enzymes. In addition, it was observed that AChE, BChE, and GST enzyme-ligands based on privileged structures contained various substituted groups which are linked with a less conserved part of the binding pocket for the enzyme selectivity. The 2-methylindole molecules bearing various sub-

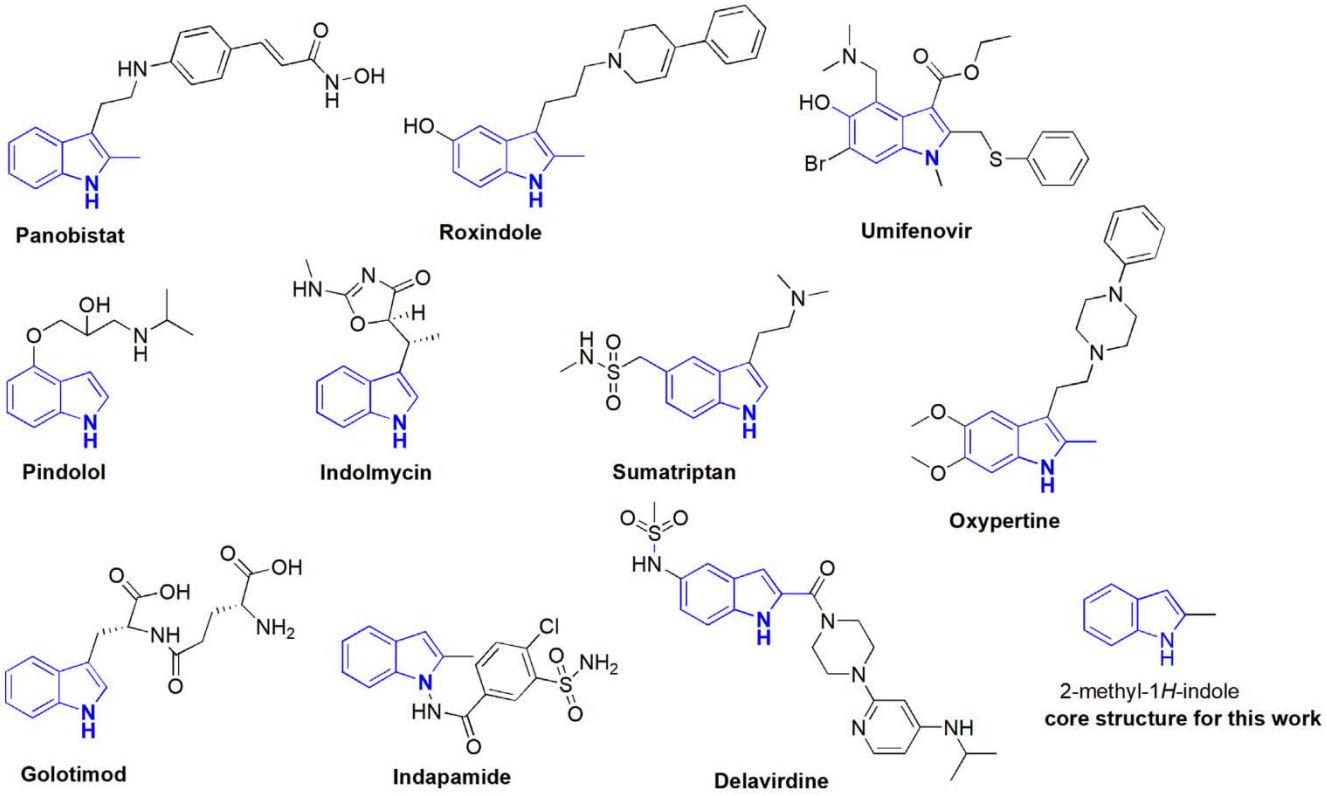

Fig. 1 Indole-containing commercial drugs.

stituents in the indole 3-position were predicted to bind these enzymes. The designed indole molecules were specified for their inhibitory effects on these enzymes.

2. Experimental methods

2.1. General

All of the chemicals, solvents, and enzymes were purchased from either Merck or Sigma-Aldrich companies. Enzymes sources from different organisms were used for the inhibition studies. Acetylcholinesterase (Electric ell AChE, EC 3.1.1.7), butyrylcholinesterase (equine serum BChE, EC 3.1.1.8), and glutathione S-transferase (human placenta GST, 2.5.1.18) were purchased from Sigma-Aldrich (Sternheim, Germany). The reagents and solvents were utilized without further purification. The progress of reactions was monitored by thin-layer chromatography (TLC) analysis on Merck pre-coated silica gel 60 F254 aluminum sheets, visualized by UV light. Melting points were recorded on an Electrothermal Gallenkamp apparatus and are uncorrected. ^{1}H and ^{13}C NMR spectra were recorded on a Varian Mercury-400 High-performance Digital FT-NMR Spectrophotometer (*Varian*, Fort Collins, CO, USA) at 400 MHz and 100 MHz, respectively. During the measurements, tetramethylsilane (TMS) was used as internal standard and deuterated $CDCl_3$ as the solvent. The chemical shifts are reported in parts per million (ppm, δ) downfield from TMS. The following abbreviations are used; singlet (s), doublet (d), triplet (t), quartet (q), multiplet (m), and broad (br s). HPLC was performed on the Shimadzu LC-20 system (Shimadzu, Japan) and a diode array detector SPD-M20A (190–800 nm) was utilized. HRMS spectra were taken on a time of flight MS system coupled to an analytical ESI detector.

2.2. Synthesis of 2-chloro-1-(2-methyl-1H-indol-3-yl)ethanone (2)

The starting compounds of this study 2-methyl-1*H*-indole (**1**) (0.13 g, 1 mmol) and pyridine (0.08 mL, 1 mmol) were dissolved in anhydrous toluene (2.5 mL). The solution was heated to 60 °C under heavy stirring. Chloroacetyl chloride (0.08 mL, 1 mmol) was added dropwise over 1 h. The reaction process was stirred for an additional 4 h. The solution was allowed to warm to room temperature and water (30 mL) and MeOH (5 mL) were added under stirring. The reaction process was filtered. The solvent was evaporated and the crude product was purified by silica gel column chromatography (n-Hexane: Ethyl acetate, 5:1) as a white powder (0.14 g, 68%). R_f 0.30 (40% EtOAc in n-heptane, v/v). mp (°C): 212–214. FTIR (cm^{-1}): 3184, 1652, 1444. ^{1}H NMR (400 MHz, $CDCl_3$): δ 9.91 (br s, 1H, NH), 7.81 (d, J = 8.0 Hz, 1H, indole-H4), 7.49 (ddd, J = 8.0, 1.2, 0.9 Hz, 1H, indole-H7), 7.25 (ddd, J = 8.2, 7.6, 1.4 Hz, 1H, indole-H6), 7.11 (ddd, J = 8.4, 7.2, 1.0 Hz, 1H, indole-H5), 4.12 (s, 2H, CH_2), 2.01 (s, 3H, CH_3); ^{13}C NMR (100 MHz, $CDCl_3$) δ 191.3 (C═O), 138.8 (indole-C7a), 131.9 (indole-C2), 128.9 (indole-C3a), 128.6 (indole-C6), 127.7 (indole-C5), 123.4 (indole-C4), 120.4 (indole-C3), 112.2 (indole-C7), 41.08 (CH_2), 21.0 (—CH_3); HPLC: R_T: 5.00 min. HRMS (ESI) Calcd. for $C_{11}H_{10}ClNONa$ [M + Na]$^+$: 230.0349; found: 230.0332.

2.3. General procedure for the synthesis of indole analogs (**4a-4j**)

Indole **2** (0.103 g, 0.5 mmol), $NaHCO_3$ (1 mmol, 0.84 mg) and NaI (0.25 g, 1 mmol) were added to a 4 mL vial. After addition of 2 mL THF and amine (0.5 mmol) was added to mixture and the resulting suspension was stirred at 60 °C for 6 h. Then 1 mL of 1 M Na_2CO_3-solution was carefully added, the mixture filtered and the filter residue washed with EtOAc. The water was added in solution. The organic phase was separated and the aqueous phase extracted with EtOAc (3 × 5 mL) and the organic phase was separated and dried over Na_2SO_4, filtered. The crude product was purified by silica gel column chromatography (n-Hexane: Ethyl acetate, 6:1) as white solid.

2.3.1. Synthesis of 2-(ethylamino)-1-(2-methyl-1H-indol-3-yl) ethanone (4a)

Yield: 49%. R_f 0.25 (40% EtOAc in n-heptane, v/v). mp (°C): 153–155. FTIR (cm^{-1}): 3182, 2954, 1630, 1558, 1442. ^{1}H NMR (400 MHz, $CDCl_3$): δ 10.01 (br s, 1H, NH), 7.74 (d, J = 8.0 Hz, 1H, indole-H4), 7.56 (ddd, J = 8.0, 1.2, 0.9 Hz, 1H, indole-H7), 7.43 (ddd, J = 8.2, 7.6, 1.4 Hz, 1H, indole-H6), 7.34 (ddd, J = 8.4, 7.2, 1.0 Hz, 1H, indole-H5), 3.96 (s, 2H, CH_2), 2.65–2.61 (m, 2H, CH_2), 2.17 (s, 3H, CH_3), 1.55 (br s, 1H, NH), 1.26 (s, 3H, CH_3); ^{13}C NMR (100 MHz, $CDCl_3$) δ 191.8 (C═O), 137.0 (indole-C7a), 130.0 (indole-C2), 128.7 (indole-C3a), 127.9 (indole-C6), 126.6 (indole-C5), 125.9 (indole-C4), 122.1 (indole-C3), 111.6 (indole-C7), 60.0, 43.8 (CH_2), 18.8, 14.3 (CH_3); HPLC: R_T: 5.68 min. HRMS (ESI) Calcd. for $C_{13}H_{16}N_2ONa$ [M + Na]$^+$: 239.1155; found: 239.1161.

2.3.2. Synthesis of 2-(tert-butylamino)-1-(2-methyl-1H-indol-3-yl)ethanone (4b)

Yield: 43%. R_f 0.25 (40% EtOAc in n-heptane, v/v). mp (°C): 169–171. FTIR (cm^{-1}): 3210, 2952, 1632, 1444. ^{1}H NMR (400 MHz, $CDCl_3$): δ 10.21 (br s, 1H, NH), 7.53 (d, J = 8.0 Hz, 1H, indole-H4), 7.45 (ddd, J = 8.0, 1.2, 0.9 Hz, 1H, indole-H7), 7.31 (ddd, J = 8.2, 7.6, 1.4 Hz, 1H, indole-H6), 7.18 (ddd, J = 8.4, 7.2, 1.0 Hz, 1H, indole-H5), 3.49 (s, 2H, CH_2), 2.56–2.54 (br s, 1H, NH), 2.02 (s, 3H, CH_3), 1.47 (s, 9H, CH_3); ^{13}C NMR (100 MHz, $CDCl_3$) δ 192.3 (C═O), 135.2 (indole-C7a), 131.1 (indole-C2), 129.5 (indole-C3a), 126.8 (indole-C6), 125.8 (indole-C5), 120.8 (indole-C4), 119.4 (indole-C3), 110.6 (indole-C7), 57.5 (CH_2), 55.2 (C-(CH_3)$_3$), 22.9, 18.5 (CH_3); HPLC: R_T: 4.71 min. HRMS (ESI) Calcd. for $C_{15}H_{20}N_2ONa$ [M + Na]$^+$: 267.1468; found: 267.1474.

2.3.3. Synthesis of 2-(benzylamino)-1-(2-methyl-1H-indol-3-yl) ethanone (4c)

Yield: 58%. R_f 0.28 (40% EtOAc in n-heptane, v/v). mp (°C): 193–195. FTIR (cm^{-1}): 3196, 3062, 2923, 1618, 1432. ^{1}H NMR (400 MHz, $CDCl_3$): δ 10.07 (br s, 1H, NH), 8.07 (d, J = 8.0 Hz, 1H, indole-H4), 7.62–7.20 (m, 5H, PhH), 7.49 (ddd, J = 8.0, 1.2, 0.9 Hz, 1H, indole-H7), 7.32 (ddd, J = 8.2, 7.6, 1.4 Hz, 1H, indole-H6), 7.26 (ddd, J = 8.4, 7.2, 1.0 Hz, 1H, indole-H5), 4.10 (d, J = 5.2 Hz, 2H, CH_2), 3.42 (d, J = 5.4 Hz, 2H, CH_2), 2.30–2.27 (br s, 1H, NH), 1.93 (s, 3H, CH_3); ^{13}C NMR (100 MHz, $CDCl_3$) δ 192.7 (C═O), 136.0 (Ph-C), 133.4 (indole-C7a), 130.5 (indole-C2), 129.8–

115.2 (5xPh-CH), 128.9 (indole-C3a), 123.8 (indole-C6), 119.2 (indole-C5), 115.2 (indole-C4), 114.1 (indole-C3), 111.8 (indole-C7), 62.7, 56.0 (—CH_2), 20.0 (—CH_3); HPLC: R_T: 4.96 min. HRMS (ESI) Calcd. for $C_{18}H_{18}N_2ONa$ [M + Na]$^+$: 301.1311; found: 301.1319.

*2.3.4. Synthesis of 1-(2-methyl-1H-indol-3-yl)-2-(pyrrolidin-1-yl)ethanone (**4d**)*

Yield: 63%. R_f 0.25 (40% EtOAc in n-heptane, v/v). mp (°C): 167–169. FTIR (cm^{-1}): 3210, 2951, 1634, 1447. ^{1}H NMR (400 MHz, $CDCl_3$): δ 9.96 (br s, 1H, NH), 7.61 (d, J = 8.0 Hz, 1H, indole-H4), 7.34 (ddd, J = 8.0, 1.2, 0.9 Hz, 1H, indole-H7), 7.17 (ddd, J = 8.2, 7.6, 1.4 Hz, 1H, indole-H6), 7.09 (ddd, J = 8.4, 7.2, 1.0 Hz, 1H, indole-H5), 4.09 (s, 2H, CH_2), 3.23 (s, 4H, CH_2), 2.19 (s, 3H, CH_3), 1.96 (s, 4H, CH_2); ^{13}C NMR (100 MHz, $CDCl_3$) δ 191.0 (C═O), 139.0 (indole-C7a), 132.8 (indole-C2), 131.2 (indole-C3a), 128.8 (indole-C6), 127.8 (indole-C5), 123.9 (indole-C4), 120.9 (indole-C3), 112.3 (indole-C7), 53.1 (CH_2), 46.3 ($N(CH_2)_2$), 26.3 (pyrrolidine-$(CH_2)_2$), 20.6 (—CH_3); HPLC: R_T: 4.21 min. HRMS (ESI) Calcd. for $C_{15}H_{18}N_2ONa$ [M + Na]$^+$: 265.1311; found: 265.1318.

*2.3.5. Synthesis of 1-(2-methyl-1H-indol-3-yl)-2-(piperidin-1-yl)ethanone (**4e**)*

Yield: 60%. R_f 0.25 (45% EtOAc in n-heptane, v/v). mp (°C): 175. ^{1}H NMR (400 MHz, $CDCl_3$): δ 10.05 (br s, 1H, NH), 7.64 (d, J = 8.0 Hz, 1H, indole-H4), 7.45 (ddd, J = 8.0, 1.2, 0.9 Hz, 1H, indole-H7), 7.26 (ddd, J = 8.2, 7.6, 1.4 Hz, 1H, indole-H6), 7.05 (ddd, J = 8.4, 7.2, 1.0 Hz, 1H, indole-H5), 4.07 (s, 2H, CH_2), 3.23 (t, J = 5.6 Hz, 4H, CH_2), 1.97 (s, 3H, CH_3), 1.81–1.78 (m, 4H, CH_2), 1.54–1.50 (m, 2H, CH_2); ^{13}C NMR (100 MHz, $CDCl_3$) δ 191.1 (C═O), 139.9 (indole-C7a), 131.1 (indole-C2), 128.1 (indole-C3a), 125.5 (indole-C6), 124.1 (indole-C5), 121.1 (indole-C4), 119.7 (indole-C3), 111.0 (indole-C7), 50.8 (CH_2), 47.8 (CH_2), 26.9 (CH_2), 24.2 (CH_2), 20.2 (—CH_3); HPLC: R_T: 5.58 min. HRMS (ESI) Calcd. for $C_{11}H_{16}N_3ONa$ [M + Na]$^+$: 229.1186; found: 229.1191.

*2.3.6. Synthesis of 1-(2-methyl-1H-indol-3-yl)-2-morpholinoethanone (**4f**)*

Yield: 66% (Mutschler and Winkler, 1978), R_f 0.25 (40% EtOAc in n-heptane, v/v). mp (°C): 191–193. FTIR (cm^{-1}): 3221, 2918, 1628, 1442, 1115. ^{1}H NMR (400 MHz, $CDCl_3$): δ 10.14 (br s, 1H, NH), 7.74 (d, J = 8.0 Hz, 1H, indole-H4), 7.49 (ddd, J = 8.0, 1.2, 0.9 Hz, 1H, indole-H7), 7.40 (ddd, J = 8.2, 7.6, 1.4 Hz, 1H, indole-H6), 7.25 (ddd, J = 8.4, 7.2, 1.0 Hz, 1H, indole-H5), 4.05–4.00 (m, 4H, $O(CH_2)_2$), 3.89 (s, 2H, CH_2), 3.80–3.76 (m, 4H, $N(CH_2)_2$), 1.98 (s, 3H, CH_3); ^{13}C NMR (100 MHz, $CDCl_3$) δ 191.9 (C═O), 131.4 (indole-C7a), 129.8 (indole-C2), 128.0 (indole-C3a), 126.2 (indole-C6), 124.1 (indole-C5), 121.3 (indole-C4), 118.9 (indole-C3), 111.4 (indole-C7), 66.1 (CH_2), 62.1 ($O(CH_2)_2$), 49.6 ($N(CH_2)_2$), 20.7 (—CH_3); HPLC: R_T: 5.68 min. HRMS (ESI) Calcd. for $C_{15}H_{18}N_2O_2Na$ [M + Na]$^+$:281.1260; found: 281.1265.

*2.3.7. Synthesis of 2-(diisopropylamino)-1-(2-methyl-1H-indol-3-yl)ethanone (**4g**)*

Yield: 40%. R_f 0.30 (50% EtOAc in n-heptane, v/v). mp (°C): 176–178. FTIR (cm^{-1}): 3234, 2956, 1615, 1438. ^{1}H NMR (400 MHz, $CDCl_3$): δ 10.13 (br s, 1H, NH), 7.84 (d, J = 8.0 Hz, 1H, indole-H4), 7.68 (ddd, J = 8.0, 1.2, 0.9 Hz, 1H, indole-H7), 7.45 (ddd, J = 8.2, 7.6, 1.4 Hz, 1H, indole-H6), 7.37 (ddd, J = 8.4, 7.2, 1.0 Hz, 1H, indole-H5), 4.06 (s, 2H, CH_2), 3.19–3.17 (m, 2H, CH), 2.00 (s, 3H, CH_3), 1.23 (s, 12H, CH_3); ^{13}C NMR (100 MHz, $CDCl_3$) δ 192.3 (C═O), 137.5 (indole-C7a), 128.3 (indole-C2), 127.3 (indole-C3a), 126.5 (indole-C6), 124.5 (indole-C5), 122.3 (indole-C4), 119.7 (indole-C3), 111.9 (indole-C7), 58.2 (CH_2), 42.4 (CH), 21.9, 18.18 (CH_3); HPLC: R_T: 5.68 min. HRMS (ESI) Calcd. for $C_{17}H_{24}N_2ONa$ [M + Na]$^+$: 295.1781; found: 295.1789.

*2.3.8. Synthesis of 1-(2-methyl-1H-indol-3-yl)-2-(phenylamino)ethanone (**4h**)*

Yield: 55%. R_f 0.30 (50% EtOAc in n-heptane, v/v). Mp (°C): 176–178. FTIR (cm^{-1}): 3228, 3062, 2943, 1621, 1443. ^{1}H NMR (400 MHz, $CDCl_3$): δ 10.45 (br s, 1H, NH), 7.71 (d, J = 8.0 Hz, 1H, indole-H4), 7.42–6.76 (m, 5H, PhH), 7.39 (ddd, J = 8.0, 1.2, 0.9 Hz, 1H, indole-H7), 7.14 (ddd, J = 8.2, 7.6, 1.4 Hz, 1H, indole-H6), 7.01 (ddd, J = 8.4, 7.2, 1.0 Hz, 1H, indole-H5), 4.17 (s, 2H, CH_2), 3.97–3.94 (br s, 1H, NH), 2.66 (s, 3H, CH_3); ^{13}C NMR (100 MHz, $CDCl_3$) δ 192.0 (C═O), 145.8 (Ph-C), 139.5 (indole-C7a), 133.9 (indole-C2), 131.4–114.3 (5xPh-CH), 127.6 (indole-C3a), 122.1 (indole-C6), 119.9 (indole-C5), 117.0 (indole-C4), 117.0 (indole-C3), 111.7 (indole-C7), 57.5 (—CH_2), 20.3 (—CH_3); HPLC: R_T: 5.68 min. HRMS (ESI) Calcd. for $C_{17}H_{16}N_2ONa$ [M + Na]$^+$: 287.1155; found: 287.1159.

*2.3.9. Synthesis of 2-(3-methoxyphenylamino)-1-(2-methyl-1H-indol-3-yl)ethanone (**4i**)*

Yield: 30%. R_f 0.28 (45% EtOAc in n-heptane, v/v). mp (°C): 188–190. FTIR (cm^{-1}): 3232, 3061, 2952, 1634, 1448, 1110. ^{1}H NMR (400 MHz, $CDCl_3$): δ 10.73 (br s, 1H, NH), 7.61 (d, J = 8.0 Hz, 1H, indole-H4), 7.45 (ddd, J = 8.0, 1.2, 0.9 Hz, 1H, indole-H7), 7.43–6.92 (m, 4H, PhH), 7.25 (ddd, J = 8.2, 7.6, 1.4 Hz, 1H, indole-H6), 7.10 (ddd, J = 8.4, 7.2, 1.0 Hz, 1H, indole-H5), 4.03 (d, J = 5.2, 2H, CH_2), 3.81 (t, J = 2.4 1H, NH), 3.35 (s, 3H, CH_3), 1.98 (s, 3H, CH_3); ^{13}C NMR (100 MHz, $CDCl_3$) δ 193.4 (C═O), 159.4, 147.0 (Ph-C), 134.6 (indole-C7a), 131.0 (indole-C2), 129.9–108.9 (4xPh-CH), 128.4 (indole-C3a), 126.8 (indole-C6), 123.1 (indole-C5), 121.7 (indole-C4), 118.7 (indole-C3), 109.7 (indole-C7), 58.5 (—CH_2), 56.8 (—OCH_3), 20.6 (—CH_3); HPLC: R_T: 5.03 min. HRMS (ESI) Calcd. for $C_{18}H_{18}N_2O_2Na$ [M + Na]$^+$: 317.1260; found: 317.1265.

*2.3.10. Synthesis of 2-(m-toluidino)-1-(2-methyl-1H-indol-3-yl)ethanone (**4j**)*

Yield: 24%. R_f 0.30 (40% EtOAc in n-heptane, v/v). mp (°C): 185. FTIR (cm^{-1}): 3229, 3060, 2946, 1632, 1444. ^{1}H NMR (400 MHz, $CDCl_3$): δ 10.49 (br s, 1H, NH), 7.63 (d, J = 8.0 Hz, 1H, indole-H4), 7.55 (ddd, J = 8.0, 1.2, 0.9 Hz, 1H, indole-H7), 7.49–6.97 (m, 4H, PhH), 7.26 (ddd, J = 8.2, 7.6, 1.4 Hz, 1H, indole-H6), 7.14 (ddd, J = 8.4, 7.2, 1.0 Hz, 1H, indole-H5), 4.10 (d, J = 5.2 Hz, 2H, CH_2), 3.72 (t, J = 2.0 Hz, 1H, NH), 2.39 (s, 3H, CH_3), 2.06 (s, 3H, CH_3); ^{13}C NMR (100 MHz, $CDCl_3$) δ 193.0 (C═O), 146.8, 140.3 (Ph-C), 135.1 (indole-C7a), 130.5 (indole-C2), 128.3–111.8 (4xPh-CH), 127.9 (indole-C3a), 126.5 (indole-C6), 123.4 (indole-C5), 121.5 (indole-C4), 116.0 (indole-C3), 109.6

(indole-C7), 58.5 (—CH_2), 33.3, 20.2 (—CH_3); HPLC: R_T: 4.76 min. HRMS (ESI) Calcd. for $C_{18}H_{18}N_2ONa$ $[M + Na]^+$:301.1311; found: 301.1319.

2.4. AChE, BChE, and GST enzyme activity methods

Cholinesterase inhibitions of the synthesized analogs were carried out according to Ellman's method with some slight modifications by using AChE and BChE enzymes (Ellman et al., 1961). The tacrine compound was used as a positive standard to compare the AChE/BChE inhibition. Briefly, 100 µL buffer solution (pH 8.0, Tris-HCl, 1.0 M), 800 µL purified water, 10 µL compound solution, and 50 µL DTNB (5,5′-dithiobis 2-nitrobenzoic) were mixed with 10 µL (10 EU) AChE/BChE enzyme solutions, respectively. After the incubation of the mixtures for 20 min, 50 µL substrates (acetylthiocholine iodide or butyrylcholine iodide) were added to the mixtures. Finally, the absorbance differences for 3 min were measured at 412 nm. GST enzyme inhibitory activities of the synthesized analogs were determined according to a previous study (Aras et al., 2019). Ethacrynic acid was used as a positive standard to compare the GST inhibition. Briefly, different concentrations (20–100 µM) of the samples in phosphate buffer (pH 6.5), GST enzyme solution (20 mM), and CDNB substrate solution (25 mM) were added to the test tubes, respectively. After the incubation of the mixtures for 20 min, GST enzyme inhibitions of the compounds were analyzed by measuring the absorbance changes for 3 min at 340 nm (Habig et al., 1974).

In the enzyme studies, one enzyme unit (EU) refers to the enzyme amount that catalyzes the conversion of 1 µmol substrate to the product in one minute duration. The enzyme kinetic studies were performed using a UV/vis spectrophotometer. For this aim, the absorbance of the control sample (without adding the tested compound) was measured and accepted to be 100% activity. The absorbance of the other samples prepared with adding different concentrations of the inhibitors were measured and their activities were calculated. The reducing activity shows the inhibition potential of a sample. The enzyme activity-concentration graphs were drawn for each tested compound. Then, the IC_{50} values (the concentration of an inhibitor to reduce 50% of enzyme activity) were calculated by using the graphic equation. The K_i values were calculated using Lineweaver-Burk graphs obtained from measurements of five different substrate concentrations.

2.5. Docking methodology

The three-dimensional X-ray crystal structures of AChE (PDB code: 4MOE), BChE (PDB code: 5NNO), and GST (PDB code: 3DK9) were retrieved in pdb format from Protein Data Bank with resolution 2.00 Å, 2.50 Å, and 0.95 Å, respectively. The structures of AChE, BChE, and GST enzymes in complex with an inhibitor were prepared by using the BIOVIA Discovery Studio software (Rao et al., 2020). The complex structures between the enzymes and co-crystallized inhibitors were illustrated in Fig. 2. The 3D structures of indole molecules synthesized were drawn with Chemdraw Ultra 8 program. The 3D structures of the indole analogs were saved in a sdf format. The 3D structures of the indole analogs were converted in a pdb format using Open Babel-2.4.0 and their energy minimizations were done by the Avogadro program (Cetin, 2021).

AutoDockVina software was performed between indole analogs and AChE, BChE, GST enzymes for molecular docking analyses such as binding types, binding energies, inhibition activities, ligand efficiency, distances, and possible interactions. Molecular docking scores were set as AutoDock Tools 1.5.7 of the molecular graphics laboratory software package by keeping the analog flexible. The binding pocket coordinates were identified the best pose whose the indole molecules were docked in surface of AChE, BChE, and GST enzymes. The grid box center was adjusted with dimensions for AChE, BChE and GST enzymes (X = 9.239 Y = -59.985 and Z = 25.538 for AChE), (X = 22.829, Y = 39.805 and Z = 37.569 for BChE) and (X = 16.807 Y = 17.303 and Z = 20.702 for GST). After validation of the docking protocol, binding conformations of the indole molecules 4a-4j based on virtual screening into the active site of AChE, BChE, and GST enzymes were evaluated. The ligand efficiencies, binding energies, inhibition activities, hydrogen bonds, and bond lengths of these enzyme-indole molecules' complexes were analyzed via AutoDockVina software.

2.6. ADMET analyses

The pharmacokinetics and toxicity properties of the indole molecules were achieved using the SwissADME which is an open online tool (http://www.swissadme.ch). The ADME properties define blood–brain barrier (BBB) permeability and

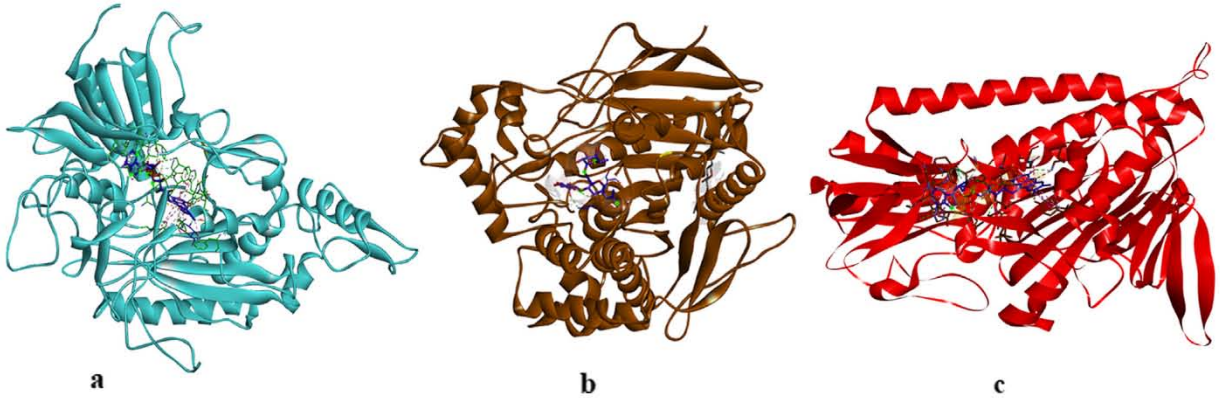

Fig. 2 The complexes between AChE, BChE, and GST with their inhibitors.

passive human gastrointestinal absorption (HIA) as well as substrate or non-substrate permeability glycoprotein (P-gp) and Cytochrome P450 (CYP) (Daina et al., 2017). Furthermore, SwissADME enables predictions for risks of toxicology such as mutagen test and carcino rat.

3. Results and discussion

3.1. Synthesis of indole analogs

Indoles are suitable tool molecules subject for pharmacological studies due to having more potent analogs of lead drugs (Singh Sidhu et al., 2016). For this aim, indole analogs were designed for the AChE, BChE, and GST enzymes suitable for *in vitro* studies by pharmacological evaluation. 2-methylindole scaffold used for the synthesis of diverse potential 3-substitued 2-methylindole molecules for the AChE, BChE, and GST. Commercially available indole **1** was utilized as starting material. That compound plays a significant role in synthesis routes based on nucleophilic substitution reactions in organic chemistry. Synthesis routes of 3-substitued 2-methylindole analogs were reported in Scheme 1. Firstly, the acylation 2-methylindole scaffold in the 3-position was synthesized using chloroacetyl chloride and pyridine according to previously published literature (Thanikachalam et al., 2019).

The synthesis approach towards analogs amine groups bearing compounds **4a-j** were prepared alkylation of various amines with molecule **2** by late-stage functionalization. Commercially acquired amines were treated with molecule **2** according to reaction conditions for alkylating amines (NaI and $NaHCO_3$), to give indole **4a-j** as shown in Scheme 1. The molecule **2** is indeed an attractive synthon. The synthesis of molecule **2** was scaled up to 5.6 g (68% yield). Application of the identified reaction conditions in THF for the indole compouns synthesis of a wide variety of primary, secondary amines including sterically hindered amine tertiary amines in yields of 24–66% as shown in Table 1. Indole **4i** and **14j** were synthesized at low yields probably thanks to the lower nucleophilicity of the amines used.

Indoles **4a** and **4b** could be isolated in overall yields of 49 and 43%. Reaction with benzylamine afforded expected product **4c** (58%). It was observed that examples the applicability of this synthesis towards more substituted 3-substitued 2-methylindole molecules. It was observed that examples the applicability of this synthesis towards more substituted 3-substitued 2-methylindole compounds in Scheme1. Indole molecules approach continue to play significant roles in the discovery of AChE, BChE, and GST enzymes (Taha et al., 2021, Kurt-Kızıldoğan et al., 2021). In this study is identified potent indole molecules based on the 2-methyl-indole scaffold were synthesized as shown Scheme 1. Organic compounds

Table 1 Scope of the reaction for synthesis of substituted indole molecules.[a]

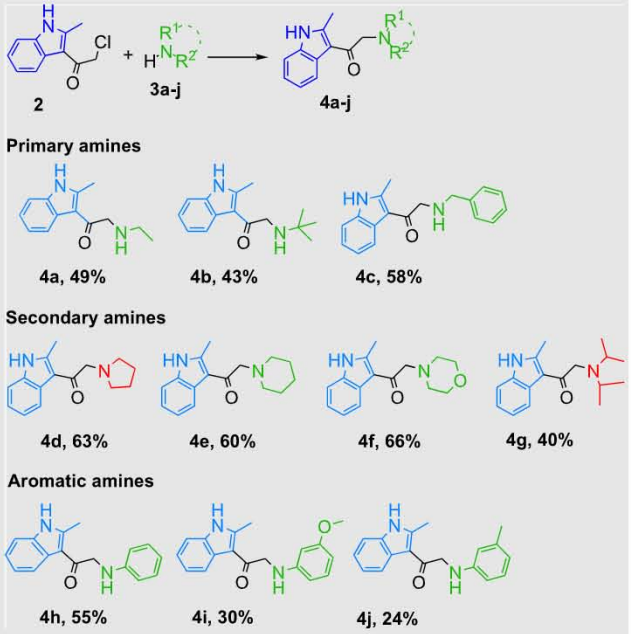

[a] Reactions were performed on a 0.5 mmol scale, using 1.0 eq. of amine in THF used as solvent at 60 °C, 8 h. Yields given are of the isolated product.

bearing amines are generally protonated at pH which increases their aqueous solubility. It was concluded that syntheses of indole molecules were obtained by aliphatic amine, aromatic amine and 2-methyl-1*H*-indole core structure. The compounds prepared had different characteristics in terms of basicity, hydrogen bonding abilities, geometry, and electronic properties. The primary, secondary and tertiary amines being able to be utilized for the synthesis of various indole molecules. The synthesized indole molecules exhibit different functional moieties and readily allows for the synthesis of functionalized indoles thereby influence both the ADMET and pharmacokinetic properties.

3.2. Enzyme inhibitory properties of indole compounds

The starting compound (**1**) and its newly synthesized molecules were evaluated for their cholinesterase and GST enzyme inhibitory activities. Remarkably, some of the compounds exhibited good inhibition activities against GST, AChE, and BChE enzymes. Ethacrynic acid was used as a positive stan-

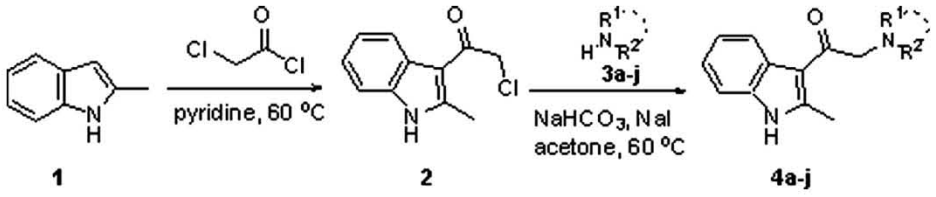

Scheme 1 Synthesis route to 2-methylindole analogs.

dard inhibitor for GST whereas tacrine was used as a positive standard inhibitor for AChE and BChE to compare the results of the synthesized molecules. The enzyme inhibitions of the compounds were determined and the results were given as IC_{50} and K_i values (Table 2). As understood from the K_i and IC_{50} values, the synthesized molecules showed a wide range of competitive, non-competitive, and semi-competitive inhibition types against the enzymes. The lower K_i and IC_{50} values indicate the more effective inhibition of the indole molecules.

According to the AChE inhibition studies, the compounds **4b** and **4i** were investigated to be the most effective inhibitors among the other newly synthesized molecules. The inhibitory potency of compound **4b** was very close to the standard compound. The K_i inhibition values of the compound **4b** and the standard tacrine were measured as 0.614 μM and 0.556 μM whereas, their IC_{50} values were calculated as 0.648 μM and 0.848 μM, respectively. In terms of the structure–activity relationship point, the AChE inhibition activity order of the synthesized indole molecules with having different substituents was found to be compound **4b** (*-tert-butylamino* group) > compound **4i** (*-3-methoxyphenylamino* group) > standard compound (*tacrine*) > compound **4j** (*-m-toluidino* group) > compound **4a** (*-ethylamino* group).

According to the BChE inhibition studies, three of the synthesized compounds (**4b**, **4a**, and **4c**) were investigated to be more effective inhibitors than the other synthesized indole molecules and the standard compound. Interestingly, the K_i inhibition values of **4b** (0.412 μM), **4a** (0.564 μM), and **4c** (0.772 μM) were found to be around half of the K_i values of tacrine (1.318 μM) that means these compounds showed more than two times BChE inhibitory activities compare to the standard tacrine compound. The IC_{50} values of the compounds **4a**, **4b**, and **4c** were found as 0.928 μM, 0.745 μM, and 1.762 μM, respectively. In terms of the structure–activity point, BChE inhibition activity order of the synthesized indole molecules with having different substituents was found to be compound **4b** (*-tert-butylamino* group) > compound **4a** (*-ethylamino* group) > compound **4c** (*-benzylamino* group) > standard compound (*tacrine*).

Remarkably, compound **4b** was found to be the most potent inhibitor of both AChE and BChE enzymes among the twelve compounds. As a comparison of the structure–activity relationship, compound **4b** is a primary amine and has a *butylamino* group on its active site. The high inhibitory potential of this compound is mainly due to hydrophobic interactions of that alkyl (butyl) group with non-polar pockets of the enzyme. A previous study reported a similar correlation and structure–activity relationship of alkyl group with the potent AChE inhibition effects of flavonol compounds (Mughal et al., 2019).

Overall, most of the tested compounds showed potent inhibitions against BChE than AChE in comparison to the standard compound. So far, many indolic compounds have been addressed for their potent AChE and BChE inhibitions in many previously published papers. For instance, one of the former studies reported the electron-donating effects of the substituents of seventeen monoterpene indole alkaloids that showed moderate to good potential for AChE inhibitions (Zhan et al., 2020). Also, another study reported that electron-donating groups afforded good to moderate BChE enzyme inhibitory activity (Shaikh et al., 2021). The structure–activity relationship analysis could help in designing new compounds for the cholinergic pathway inhibitors based on indole molecules.

The results of *in vitro* and *in silico* studies seems to have low correlations. However, the potent inhibitor compounds according to the *in vitro* enzyme studies also showed low energy levels in molecular docking studies. For instance, the most potent inhibitor for both AChE and BChE, compound **4b** determined to have low binding energy levels in molecular docking studies that proved the good interactions of the compound with the enzymes. Overall, the energy levels of the tested compounds were detected close to the standard compounds.

According to the GST inhibition studies, the starting compound **1** and compound **4i** were investigated to be the most effective GST inhibitors among the other newly synthesized molecules. The inhibition potency of the compound **1** was higher than the standard compound (ethacrynic acid) as well. The K_i inhibition values of compound **1** and standard ethacry-

Table 2 GST and cholinesterases (AChE and BChE) enzyme inhibition values of indole analogs.

İndole	IC_{50} (μM)					K_i (μM)			
	GST	R^2	AChE	R^2	BChE	R^2	GST	AChE	BChE
1	0.347	0.9822	4.482	0.9612	4.147	0.9486	0.308	3.790	4.761
2	13.970	0.9633	3.262	0.9412	4.086	0.9863	8.376	3.881	3.026
4a	10.492	0.9417	2.864	0,9148	0.928	0.9624	4.478	2.489	0.564
4b	6.143	0.9298	0.648	0.9684	0.745	0.9856	5.875	0.614	0.412
4c	0.886	0.9491	3.461	0.9842	1.762	0.9108	1.312	3.341	0.772
4d	6.748	0.9680	4.874	0.9942	4.127	0.8876	5.840	3.746	2.396
4e	0.426	0.9386	6.120	0.9784	5.726	0.9228	0.466	5.764	3.334
4f	3.485	0.9814	9.852	0.9338	6.486	0.9862	3.019	8.882	2.896
4g	10.286	0.9592	10.760	0.9482	13.856	0.9762	7.762	5.289	7.318
4h	6.328	0.9432	11.581	0.9614	9.425	0.9696	4.783	4.782	6.148
4i	0.568	0.9894	3.286	0.9845	5.749	0.9436	0.514	1.043	4.027
4j	1.745	0.9456	4.880	0.9828	5.456	0.9127	1.312	2.086	3.649
*Tacrine	–	–	0.848	0.9962	2.486	0.9028	–	**0.556**	**1.318**
** Ethacrynic acid	0.374	0.9632					**0.386**		

* Standard inhibitor for ACHE and BCHE enzymes.
** Standard inhibitor for GST enzyme.

nic acid were 0.308 μM and 0.386 μM whereas their IC_{50} values were determined as 0.347 μM and 0.374 μM, respectively. In terms of the structure–activity point, the GST inhibition activity order of the synthesized indole molecules with having different substituents was found to be compound **1** (2-methyl-1*H*-indole) > standard compound (*ethacrynic acid*) > compound **4e** (*-piperidin-1-yl* group) > compound **4i** (*-3-methoxyphenylamino* group). Similar to these results, a previous study showed the inhibition effect of an indole molecules up to a 69 % decrease in GST enzyme activity (Konus et al., 2020).

3.3. Molecular docking studies

The main interactions between indole molecules and the enzymes (AChE, BChE, and GST) such as the binding affinities, hydrogen bonds, and bond lengths etc. were obtained by using AutoDock Vina software. Moreover, ethacrynic acid a standard inhibitor of GST and tacrine as a reference drug for AChE and BChE were used for comparing the molecular docking results of the indole molecules (Cetin et al., 2021). Molecular docking is a molecular modeling technique and one of the most commonly employed methods to analyze the detailed interactions between the chemical structures of the compounds and enzymes. In case of AChE and BChE, the crystal structure of *Trametes ochracea* and *Trypanosoma brucei* available at low crystallographic resolutions was selected, respectively (Turkan et al., 2019; Türkan et al., 2021). The acetylcholine transporter of *Trametes ochracea* was chosen due to related to the catalyze the oxidation of monoamines and acted upon amino acids. Furthermore, *Trypanosoma brucei* structures create electron transport chains in the occurred complexes and an enzyme that catalyzes the transfer of electrons from one molecule. For GST, the high-resolution crystallographic structure of human glutathione reductase was selected at nominal resolutions between 1.1 and 0.95 A. Since, in addition to the properties given above,these structures catalyse the transfer of specific functional groups from electrically neutral group of two or more atoms and also, have involved hundreds of different biochemical pathways and vital processes (Türkan et al., 2021). After extraction from the respective macromolecule, the co-crystallized indole molecules of AChE, BChE and GST were docked inside the active site. Also, the re-docking of co-crystallized ligands (G3F for 4MOE and 92 N for 5NNO, and FAD for 3DK9) were carried out to validate the docking studies. The crystal poses of indole molecules were docked into the binding site of AChE, BChE, and GST enzymes with identified docking search algorithms and scoring functions. All indole molecules were docked using similar optimized docking conditions (See Figures and Tables in the Supplementary Material file). The binding energies, inhibition activities, and ligand efficiency of the indole molecules with AChE, BChE, and GST enzymes were illustrated in Table 3. Initially, the drug score, Volume $Å^3$ and Surface $Å^3$ were determined for indole molecules-AChE, BChE, and GST 0.81, 2371.25, and 3049.62, respectively. The binding affinity values of indole molecules-AChE enzyme ranged from −9.0 to −6.9 kcal/mol and their ligand efficiencies were obtained between −0.49 and −0.37. The binding affinity values of indole molecules-BChE enzyme ranged from −8.1 to −6.8 kcal/mol and their ligand efficiencies were obtained between −0.48 and −0.33 and also, the binding affinity values of indole molecules-GST ranged from −8.7 to −6.3 kcal/mol and their ligand efficiencies were obtained between −0.45 and −0.39 using AutoDock Vina. The ligand efficient values of all indole-enzyme complexes achieved close values for the enzymes used. The binding affinities of all indole-AChE complexes were found to be higher than the binding affinity value of the standard drug-AChE complex. The binding affinity (−9.0 kcal/mol) of indole 4c-AChE complex was found to be the highest among binding affinities the all indole-AChE complexes in Fig. 3. The binding affinity of indole **4j**-AChE complex was also a very close value as −8.8 kcal/mol. The binding affinities of the indole molecules **4a**, **4d**, **4f**, and **4 g** were found to be a lower value than binding affinities of the other indole molecules in the AChE activity.

The binding affinity (−8.2 kcal/mol) of indole molecule **4i** was found to be the highest value among binding affinities of the indole molecules in the BChE activities. The binding affini-

Table 3 The binding affinity and ligand efficiency of the Indole analogs into the active catalytic pocket of AChE, BChE and GST.

No	AChE-3dk9		BChE-4moe		GST-5nn0	
	Binding Affinity (kcal/mol)	Ligand Efficiency	Binding Affinity (kcal/mol)	Ligand Efficiency	Binding Affinity (kcal/mol)	Ligand Efficiency
2	−6.9	−0.49	−6.8	−0.48	−6.3	−0.45
4a	−7.6	−0.48	−6.7	−0.42	−7.1	−0.44
4b	−8.2	−0.45	−7.3	−0.41	−7.5	−0.41
4c	**−9.0**	−0.43	−7.8	−0.37	−8.4	−0.4
4d	−7.5	−0.41	−7.3	0.33	−7.7	−0.43
4e	−8.0	−0.42	−7.5	−0.4	−8.3	−0.44
4f	−7.6	−0.4	−7.0	−0.37	−7.5	−0.39
4g	−7.3	−0.37	−6.8	−0.34	−7.8	−0.39
4h	−8.3	−0.42	−7.8	−0.39	−8.3	−0.42
4i	−8.4	−0.38	**−8.2**	−0.37	**−8.6**	−0.39
4j	**−8.8**	−0.42	**−8.1**	−0.38	**−8.7**	−0.42
Tacrine	−6.4	−0.43	−7.0	−0.46	–	–
Ethacrynic acid	–	–	–	–	−7.71	−0.59

*TAC and Ethacrynic acid were used as reference drugs for AChE, BChE and GST.

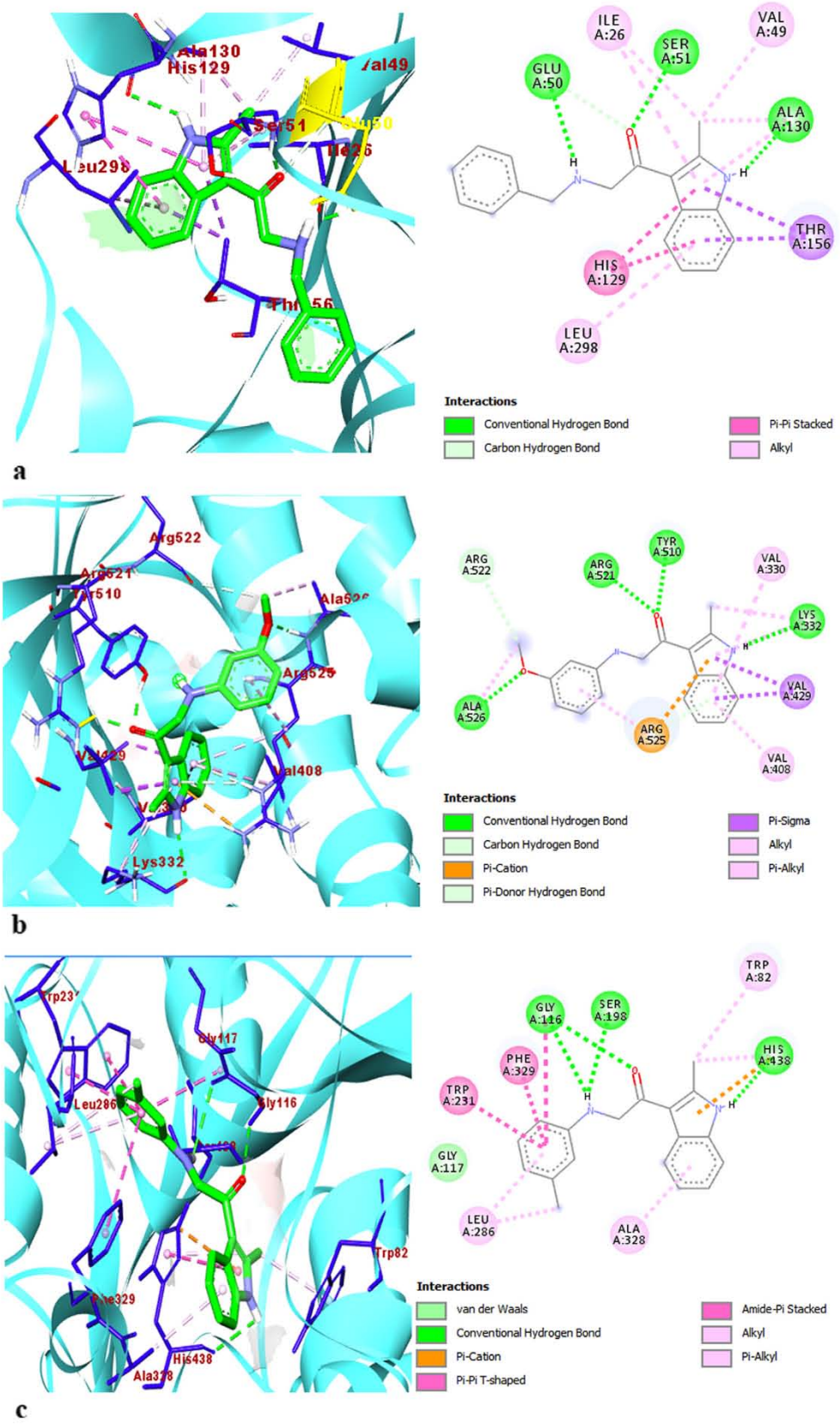

Fig. 3 The 2D and 3D interaction profiles and detailed binding mode of best-posed indole molecules into the enzymes (a) 4c-AChE, (b) 4i-BChE, and (c) 4j-GST.

ties of all indole molecules except compounds **4a** and **4g** were found to be higher values than the binding affinity of the standard drug. The binding affinities of all indole molecules except **4a**, **4b** for BChE activity and compound **4f** for GST activity were found to be higher value than the binding affinity of the standard drug. However, the binding affinities of **4b** and **4f** (−7.5 kcal/mol) were achieved close values according to the binding affinity of the standard drug (−7.7 kcal/mol) for GST activity. The binding affinity of indole molecule **4j** (−8.7 kcal/mol) was found to be the highest value among binding affinities of the other indole molecules in the GST activities (Fig. 3.). Moreover, the binding affinity of indole molecule **4i** was a very close value as −8.6 kcal/mol for GST activity. The binding affinities of the indole molecules **4c**, **4e,** and **4h** had values close to each other as −8.4, −8.3, and −8.3 kcal/-mol in the GST activities, respectively.

The indole **4j** and **4i** had good binding affinities for the enzymes used. This is thought to be due to the substituents attached to the phenyl ring at the meta position of the **4j** and **4i** indole compounds (Konus et al., 2020). The molecular docking results of the indole-enzyme complexes were revealed that, all indole-enzyme complexes showed π-alkyl interactions with Lys332, Val429, Tyr510, Arg525, Ala397, Leu394, Val330 residues in the active site of the AChE, Phe329, Leu286, Ala328, Trp82, His438, Pro84 residues in the active sites in the BChE, and Ala342, Cys58, Cys63, Ala130, Leu298, Ile26, Val49 residues in the active sites in the GST, respectively (Table 4 and Supp. Mater. Tables S1-S3) The indole molecules **4d** and **4f** showed Van der Waals in the hydrophobic bonding types with Thr383 residue in the active site of the AChE. The indole molecules **4h**, **4i**, and **4j** showed Van der Waals in the hydrophobic bonding type with Gly117 residue in the active site of the BChE enzyme. The indole molecules **4a**, **4h**, and **4i** also showed Van der Waals with Asn294 and Gly157 residues in the active site of the GST enzyme. In addition, all of the indole-enzyme complexes showed alkyl interactions with Ile26, Leu298, Val49, Ala130, Lys66, Ile198 residues, and Val408, Arg525, Val330, Arg393, Arg397, Lys332, Leu394 Arg383, Phe359 Ala526 residues in the active sites of the AChE and GST enzymes, respectively.

The indole compounds **4a**, **4b**, and **4c** only showed alkyl interactions with Tyr440, Met437, Trp82, Leu442, Leu286, Ile69, and Ala328 residues in the active sites of the BChE enzyme. The complex structures between the indole compounds and the AChE, BChE, and GST enzymes were stabilized by hydrogen bonds containing oxygen (-O), hydrogen (-H), and carbonyl (—C═O) moieties simultaneously as donor and acceptor with Arg521, Tyr510, Lys332, Gly523, Asp400, Arg356, Pro285, His438, Gly116, Asp70, Tyr332, Gln67, Cys58, Ser30, Asp331, Glu50, Ser51, Ala130, Gly27, Glu201, and Gly62 residues. The indole compounds except indole **4d** showed π donor hydrogen bond with Arg525 residue in the active site of the AChE. The indole compounds **4h** and **4i** showed π donor hydrogen bond with Trp82 residue in the active site of the BChE. The indole compound **4g** showed π donor hydrogen bond with Asp331 residue in the active site of the GST (Türkan et al., 2021). The indole-enzyme complexes had electronic interactions with the AChE amino acids Arg525, Val330, Val429, Val329, Ala397, and Tyr382, with the BChE amino acids Phe329, Trp231, His438, Trp430, Trp82, Gly116, and Trp231, and with the GST amino acids Asp331, His129, Thr156, Gly62, Ile198, and Gly28. The molecular docking simulations of indole molecules-enzyme complexes are given detailly in the Supplemental Material files.

3.4. Pharmacokinetic studies

Physicochemical, drug-likeness, and pharmacokinetic properties of the indole molecules **4a-j** were illustrated by the online website of SwissADME server as shown in Table 5 (Daina et al., 2017). Furthermore, drug metabolism, pharmacokinetics (ADME), and drug-induced toxicity properties of the indole compounds **4a-j** were calculated using SwissADME database. All indole compounds **4a-j** obey the Lipinski's rule of five. The indole compounds **4a-j** have a bioavailability score of 0.55 and are moderately soluble in water. Also, the mutagenicity and carcinogenicity of the indole compounds **4a-j** were evaluated using the SwissADME server (Mpiana et al., 2020). The pharmacokinetics and toxicity properties of the indole compounds **4c**, **4h**, **4i**, and **4j** with high binding energies were evaluated the potential of these compounds as drug candidates. As seen in Table 5, the transporter class P-glycoprotein (P-gp) and Cytochrome P450 (CYP) metabolic enzymes, which are important in drug metabolism, were assessed in this study. The indole **4c**, **4h**, and **4j** were found to be effective inhibitors of all CYPs except CYP2C9. The indole **4i** was found to be an inhibitor of all CYPs. The CYP inhibitors of these indole compounds are significant to explore the pharmacokinetics for preventing undesired drug-drug interactions. Indole **4c** having P-gp and

Table 4 Molecular interactions of the AChE, BChE and GST active sites with the indol analogs (**4c**, **4i**, **4j**).

Complex	Type of intreactions	İntreacting residues
AChE-4c	H-bond, π-sigma, π-cation, π-donor H bond alkyl, π-alkyl	Gly523, Arg521, Tyr510, Arg525, Lys332, Val330, Val429, Val408
AChE-4j	H-bond, π-sigma, π-cation, π-donor H bond alkyl, π-alkyl	Gly523, Tyr510, Arg521, Val429, Val430, Arg525, Val408, Ala525, Lys332
BChE-4i	H-bond, π-sigma, amide π stacked, π-π T-shaped, π-alkyl, Van Der Walls	Gly116, Trp82, His438, Trp231, Phe329, Ala328, Leu286, Gly117
BChE-4j	H-bond, π-cation, amide π stacked, π-π T-shaped, π-alkyl, alkyl, Van Der Walls	Gly116, Ser198, His438, Phe329, Trp231, Ala328, Leu286, Trp82, Gly117
GST-4i	H-bond, π-sigma, amide π stacked, π-π stacked, π-alkyl, alkyl, Van Der Walls	Glu50, Ser51, Ala130, Thr156, His129, Leu298, Ile26, Val49, Gly157
GST-4j	H-bond, π-sigma, π-π stacked, unfavorable bond, π-alkyl, alkyl	Glu50, Ser51, Ala130, Thr156, His129, Gly28, Leu298, Ile26, Val49

Table 5 Drug likeliness properties of the indol analogs using SwissADME.

	2	**4a**	**4b**	**4c**	**4d**	**4e**	**4f**	**4g**	**4h**	**4i**	**4j**
Physicochemical Properties and Druglikeness											
Molecular weight (g/mol)	207.66	*216.28*	*244.33*	*278.35*	*242.32*	*256.34*	*258.32*	*272.39*	*264.32*	*294.35*	*287.35*
Num.H-bond acceptors	1	2	2	2	2	2	3	2	1	2	1
Num. H-bond donors	1	2	2	2	1	1	1	1	2	2	2
Molar Refractivity	58.26	65.87	75.53	85.55	77.38	82.19	78.47	85.20	82.29	88.78	87.25
Log $P_{o/w}$	2.57	*2.19*	*2.72*	*3.08*	*2.51*	*2.79*	*1.94*	*3.32*	*3.18*	*3.16*	*3.45*
Log S	−4.65	−2.67	−3.32	*−3.85*	*−3.10*	*−3.47*	*−2.40*	*−4.25*	*−4.48*	*−4.64*	*−4.86*
TPSA (Å2)	32.86	*44.89*	*44.89*	*44.89*	*36.10*	*36.10*	*45.33*	*36.10*	*44.89*	*54.12*	*44.89*
Lipinski	yes	yes	yes	*yes*	*yes*	*yes*	*yes*	*yes*	*yes*	*yes*	*yes*
Bioavailability Score	0.55	0.55	0.55	0.55	*0.55*	*0.55*	*0.55*	*0.55*	*0.55*	*0.55*	*0.55*
Synthetic accessibility	1.67	*1.79*	*2.00*	*2.03*	1.93	*2.03*	*2.09*	*2.21*	*2.01*	*2.22*	*2.14*
Pharmacokinetics											
BBB permeant	yes	yes	yes	yes	yes	yes	yes	*yes*	*yes*	*yes*	*yes*
GI absorption	high	high	high	high	high	high	high	*high*	*high*	*high*	*high*
P-gp substrate	no	no	no	yes	yes	yes	yes	*no*	*no*	*no*	*no*
1A2	yes	yes	yes	yes	yes	yes	yes	*yes*	*yes*	*yes*	*yes*
2C19	yes	no	no	yes	yes	yes	yes	*yes*	*yes*	*yes*	*yes*
2C9	no	no	no	no	no	no	no	*no*	*no*	*yes*	*No*
2D6	no	no	*yes*	yes	yes	yes	yes	*yes*	*yes*	*yes*	*Yes*
3A4	no	no	no	yes	no	no	no	*no*	*yes*	*yes*	*yes*

nt = not toxic; ht = high toxic; GI:Gastrointestinal absorption; BBB: Blood brain barrier; P-gp:Permeability Glycoprotein; CYP: Cytochrome P450

CYP3A4 can be a barrier in the transmembrane transportation of drugs since both are good transporters in the intestine (Daina et al., 2017).

It was observed that the indole compounds achieved good results in terms of their BBB permeant and GI absorption properties from the SwissADME database. Since, the indole compounds **4a-j** had BBB permeant and GI absorption properties. The BBB permeant and GI absorption of the indole compounds can protect the brain and the central nervous system as well as allows molecules to enter the cell according to the size and lipid solubility of the molecules (Ramesh, et al., 2020).

4. Conclusion

In conclusion, we demonstrated the synthesis of the 2-methylindole molecules as acetylcholinesterase, butyrylcholinesterase, and glutathione S-transferase inhibitors using chemical methodologies including the alkylations and substitute amine bond formations. The synthesized indole compounds exhibited moderate to good inhibition activities against GST, AChE, and BChE enzymes. Briefly, the inhibitory activities of the compounds **4b** and **4i** against AChE, compounds **4a** and **4b** against BChE, and compounds **1** and **4i** against GST were detected to be higher or close to the standard inhibitor compounds. The molecular docking studies revealed the molecular interactions of the analyses of docking of the indole compounds with AChE, BChE, and GST enzymes. The molecular docking simulations of these complexes appeared similar complex binding conformations. The indole compounds **4c** and **4j** were observed with the residues of Glu50, Ser51, and Ala130 residues and were found to be potent inhibitor candidates which have −9.0 and −8.8 binding energy affinities (kcal/mol). The indole compounds were occurred a stable conformer and good binding site by creating aromatic, hydrogen, and hydrophobic bonds in the AChE, BChE, and GST active site residues. Furthermore, the results of ADMET and pharmacokinetic analyses suggested that the indole compounds were found in good agreement with the many accepted rules and the criteria of drug-likeness. The designed 2-methylindole compounds can be a guide to medicinal chemists within the enzyme field.

Declaration of Competing Interest

The authors declare that they have no known competing financial interests or personal relationships that could have appeared to influence the work reported in this paper.

Appendix A. Supplementary material

Supplementary data to this article can be found online at https://doi.org/10.1016/j.arabjc.2021.103449.

References

Aras, A., Bursal, E., Türkan, F., Tohma, H., Kılıç, Ö., Gülçin, İ., Köksal, E., 2019. Phytochemical content, antidiabetic, anticholinergic, and antioxidant activities of endemic Lecokia cretica extracts. Chem. Biodivers. 16,. https://doi.org/10.1002/cbdv.201900341 e1900341.

Aras, A., Türkan, F., Yildiko, U., Atalar, M.N., Kılıç, Ö., Alma, M. H., Bursal, E., 2021. Biochemical constituent, enzyme inhibitory activity, and molecular docking analysis of an endemic plant species, Thymus migricus. Chem. Pap. 75, 1133–1146. https://doi.org/10.1007/s11696-020-01375-z.

Blaising, J., Polyak, S.J., Pécheur, E.I., 2014. Arbidol as a broad-spectrum antiviral: an update. Antiviral Res. 107, 84–94. https://doi.org/10.1016/j.antiviral.2014.04.006.

Cetin, A., 2021. In silico studies on stilbenolignan analogues as SARS-CoV-2 Mpro inhibitors. Chem. Phys Lett. 771,. https://doi.org/10.1016/j.cplett.2021.138563 138563.

Cetin, A., Türkan, F., Bursal, E., Murahari, M., 2021. Synthesis, characterization, enzyme inhibitory activity, and molecular docking analysis of a new series of thiophene-based heterocyclic compounds. Russ. J. Org. Chem. 57 (4), 598–604. https://doi.org/10.1134/S107042802104014X.

Chaffman, M., Heel, R.C., Brogden, R.N., Speight, T.M., Avery, G.S., 1984. Indapamide. Drugs 28 (3), 189–235. https://doi.org/10.2165/00003495-198428030-00001.

Cheng, G., Wang, Z., Yang, J., Bao, Y., Xu, Q., Zhao, L., Liu, D., 2019. Design, synthesis and biological evaluation of novel indole derivatives as potential HDAC/BRD4 dual inhibitors and anti-leukemia agents. Bioorg. Chem. 84, 410–417. https://doi.org/10.1016/j.bioorg.2018.12.011.

Daina, A., Michielin, O., Zoete, V., 2017. SwissADME: a free web tool to evaluate pharmacokinetics, drug-likeness and medicinal chemistry friendliness of small molecules. Sci. Rep. 7, 42717. https://doi.org/10.1038/srep42717.

da Silva Guerra, A.S.H., do Nascimento Malta, D.J., Laranjeira, L.P. M., Maia, M.B.S., Colaço, N.C., de Lima, M.D.C.A., Gonçalves-Silva, T., 2011. Anti-inflammatory and antinociceptive activities of indole–imidazolidine derivatives. Int. Immunopharmacol. 11 (11), 1816–1822. https://doi.org/10.1016/j.intimp.2011.07.010.

Dechant, K.L., Clissold, S.P., 1992. Sumatriptan. Drugs 43 (5), 776–798. https://doi.org/10.2165/00003495-199243050-00010.

Demeter, L.M., Shafer, R.W., Meehan, P.M., Holden-Wiltse, J., Fischl, M.A., Freimuth, W.W., Reichman, R.C., 2000. Delavirdine susceptibilities and associated reverse transcriptase mutations in human immunodeficiency virus type 1 isolates from patients in a phase I/II trial of delavirdine monotherapy (ACTG 260). Antimicrob. Agents Chemother. 44 (3), 794–797. https://doi.org/10.1128/AAC.44.3.794-797.2000.

Dinnell, K., Elliott, J., Hollingworth, G., Ridgill, M., Shaw, D., 2001. U.S. Patent Application No. 09/782,422.

Durell, J., Pollin, W., 1963. A trial on chronic schizophrenic patients of oxypertine, a psychotropic drug with an indole ring. Br. J. Psychiatry. 109 (462), 687–691. https://doi.org/10.1192/bjp.109.462.687.

Dvořák, Z., Poulíková, K., Mani, S., 2021. Indole scaffolds as a promising class of the aryl hydrocarbon receptor ligands. Eur. J. Med. Chem. 215,. https://doi.org/10.1016/j.ejmech.2021.113231 113231.

Ellman, G.L., Courtney, K.D., Andrey Jr, V., Featherstone, R.M., 1961. A new and rapid colorimetric determination of acetylcholinesterase activity. Biochem. Pharm. 7, 88–95. https://doi.org/10.1016/0006-2952(61)90145-9.

Erlanson, D.A., de Esch, I.J., Jahnke, W., Johnson, C.N., Mortenson, P.N., 2020. Fragment-to-lead medicinal chemistry publications in 2018. J. Med. Chem. 63, 4430–4444. https://doi.org/10.1021/acs.jmedchem.9b01581.

Geiger, J.L., Grandis, J.R., Bauman, J.E., 2016. The STAT3 pathway as a therapeutic target in head and neck cancer: Barriers and innovations. Oral oncol. 56, 84–92. https://doi.org/10.1016/j.oraloncology.2015.11.022.

Gn, S.H.S., Ganesan Rajalekshmi, S., Murahari, M., Burri, R.R., 2020. Reappraisal of FDA approved drugs against Alzheimer's disease based on differential gene expression and protein interaction network analysis: an in silico approach. J. Biomol. Struct. Dyn. 38 (13), 3972–3989. https://doi.org/10.1080/07391102.2019.1671231.

Goyal, D., Kaur, A., 2018. Goyal, Benzofuran and indole: promising scaffolds for drug development in Alzheimer's disease. ChemMedChem. 13 (13), 1275–1299. https://doi.org/10.1002/cmdc.201800156.

Grochowski, D.M., Uysal, S., Aktumsek, A., Granica, S., Zengin, G., Ceylan, R., Tomczyk, M., 2017. In vitro enzyme inhibitory properties, antioxidant activities, and phytochemical profile of Potentilla thuringiaca. Phytochem. Lett. 20, 365–372. https://doi.org/10.1016/j.phytol.2017.03.005.

Gurkok, G., Altanlar, N., Suzen, S., 2009. Investigation of antimicrobial activities of indole-3-aldehyde hydrazide/hydrazone derivatives. Chemotherapy. 55 (1), 15–19. https://doi.org/10.1159/000166999.

Habig, W.H., Pabst, M.J., Jakoby, W.B., 1974. Glutathione S-transferases. The first enzymatic step in mercapturic acid formation. J. Biol. Chem. 249, 7130–7139. https://doi.org/10.1016/S0021-9258(19)42083-8.

Hamid, H.A., Ramli, A.N., Yusoff, M.M., 2017. Indole alkaloids from plants as potential leads for antidepressant drugs: A mini review. Front. Pharmacol. 8, 96. https://doi.org/10.3389/fphar.2017.00096.

Harnden, M.R., Bailey, S., Boyd, M.R., Taylor, D.R., Wright, N.D., 1978. Thiazolinone analogs of indolmycin with antiviral and antibacterial activity. J. Med. Chem. 21 (1), 82–87. https://doi.org/10.1021/jm00199a015.

Kasper, S., Fuger, J., Zinner, H.J., Bäuml, J., Möller, H.J., 1992. Early clinical results with the neuroleptic roxindole (EMD 49 980) in the treatment of schizophrenia-an open study. Eur. Neuropsychopharmacol. 2 (1), 91–95. https://doi.org/10.1016/0924-977X(92)90041-6.

Konus, M., Çetin, D., Yılmaz, C., Arslan, S., Mutlu, D., Kurt-Kızıldoğan, A., Kivrak, A., 2020. Synthesis, biological evaluation and molecular docking of novel thiophene-based indole derivatives as potential antibacterial, GST inhibitor and apoptotic anticancer agents. ChemistrySelect. 5 (19), 5809–5814. https://doi.org/10.1002/slct.202001523.

Kurt-Kızıldoğan, A., Otur, Ç., Yılmaz, C., Arslan, S., Mutlu, D., Kivrak, A., Konus, M., 2021. Synthesis, cytotoxicity, antioxidant and antimicrobial activity of indole based novel small molecules. Lett. Drug Des. Discov. 18 (5), 461–470. https://doi.org/10.2174/1570180817999201109203226.

Makhaeva, G.F., Lushchekina, S.V., Boltneva, N.P., Sokolov, V.B., Grigoriev, V.V., Serebryakova, O.G., Bachurin, S.O., 2015. Conjugates of γ-Carbolines and Phenothiazine as new selective inhibitors of butyrylcholinesterase and blockers of NMDA receptors for Alzheimer Disease. Sci. Rep. 5 (1), 1–11. https://doi.org/10.1038/srep13164.

Morgan, A.S., Ciaccio, P.J., Tew, K.D., Kauvar, L.M., Ciaccio, F.J., 1996. Isozyme-specific glutathione S-transferase inhibitors potentiate drug sensitivity in cultured human tumor cell lines. Cancer Chemother. Pharmacol. 37 (4), 363–370. https://doi.org/10.1007/s002800050398.

Mpiana, P.T., Tshibangu, D.S., Kilembe, J.T., Gbolo, B.Z., Mwanangombo, D.T., Inkoto, C.L., Tshilanda, D.D., 2020. Identification of potential inhibitors of SARS-CoV-2 main protease from Aloe vera compounds: a molecular docking study. Chem. Phys. Lett. 754,. https://doi.org/10.1016/j.cplett.2020.137751 137751.

Mughal, E.U., Sadiq, A., Ashraf, J., Zafar, M.N., Sumrra, S.H., Tariq, R., Javed, C.O., 2019. Flavonols and 4-thioflavonols as potential acetylcholinesterase and butyrylcholinesterase inhibitors: Synthesis, structure-activity relationship and molecular docking studies. Bioorg. Chem. 91,. https://doi.org/10.1016/j.bioorg.2019.103124 103124.

Mughal, E.U., Sadiq, A., Ayub, M., Naeem, N., Javid, A., Sumrra, S. H., Ahmed, I., 2020. Exploring 3-Benzyloxyflavones as new lead cholinesterase inhibitors: synthesis, structure-activity relationship and molecular modelling simulations. J. Biomol. Struct. Dyn. 1–14. https://doi.org/10.1080/07391102.2020.1803136.

Mumtaz, A., Majeed, A., Zaib, S., Rahman, S.U., Hameed, S., Saeed, A., Iqbal, J., 2019. Investigation of potent inhibitors of cholinesterase based on thiourea and pyrazoline derivatives: Synthesis, inhibition assay and molecular modeling studies. Bioorg. Chem. 90,. https://doi.org/10.1016/j.bioorg.2019.103036 103036.

Mutschler, E., Winkler, W., 1978. Über lokalanästhetisch und antiarrhythmisch wirksame Indol-und Indolin-Derivate, 1. Mitt. Darstellung von 1-,2-und 3-Aminoacetyl-indolen sowie 1-

Aminoacetylindolinen. Arch. Pharm. 311 (3), 248–255. https://doi.org/10.1002/ardp.19783110311.

Ramesh, D., Joji, A., Vijayakumar, B.G., Sethumadhavan, A., Mani, M., Kannan, T., 2020. Indole chalcones: Design, synthesis, in vitro and in silico evaluation against Mycobacterium tuberculosis. Eur. J. Med. Chem. 198,. https://doi.org/10.1016/j.ejmech.2020.112358 112358.

Rao, P., Shukla, A., Parmar, P., Rawal, R.M., Patel, B., Saraf, M., Goswami, D., 2020. Reckoning a fungal metabolite, Pyranonigrin A as a potential Main protease (Mpro) inhibitor of novel SARS-CoV-2 virus identified using docking and molecular dynamics simulation. Biophys. Chem. 264,. https://doi.org/10.1016/j.bpc.2020.106425 106425.

Roberts, D., Mcloughlin, G., Tsao, Y., Breckenridge, A., 1987. Placebo-controlled comparison of captopril, atenolol, labetalol, and pindolol in hypertension complicated by intermittent claudication. Lancet 330 (8560), 650–653. https://doi.org/10.1016/S0140-6736(87)92441-X.

Schultz, M., Dutta, S., Tew, K.D., 1997. Inhibitors of glutathione S-transferases as therapeutic agents. Adv. Drug Deliv. Rev. 26 (2–3), 91–104. https://doi.org/10.1016/S0169-409X(97)00029-X.

Shaikh, S., Pavale, G., Dhavan, P., Singh, P., Uparkar, J., Vaidya, S. P., Ramana, M.M.V., 2021. Design, synthesis and evaluation of dihydropyranoindole derivatives as potential cholinesterase inhibitors against Alzheimer's disease. Bioorg. Chem. 110,. https://doi.org/10.1016/j.bioorg.2021.104770 104770.

Singh, A.A., Patil, M.P., Kang, M.J., Niyonizigiye, I., Kim, G.D., 2021a. Biomedical application of Indole-3-carbinol: A mini-review. Phytochem. Lett. 41, 49–54. https://doi.org/10.1016/j.phytol.2020.09.024.

Singh, Y.P., Rai, H., Singh, G., Singh, G.K., Mishra, S., Kumar, S., Modi, G., 2021b. A review on ferulic acid and analogs based scaffolds for the management of Alzheimer's disease. Eur. J. Med. Chem. 215,. https://doi.org/10.1016/j.ejmech.2021.113278 113278.

Singh Sidhu, J., Singla, R., Jaitak, V., 2016. Indole derivatives as anticancer agents for breast cancer therapy: a review. Anti-Cancer Agents Med. Chem. 16 (2), 160–173.

Solangi, M., Khan, K.M., Saleem, F., Hameed, S., Iqbal, J., Shafique, Z., Perveen, S., 2020. Indole acrylonitriles as potential anti-hyperglycemic agents: Synthesis, α-glucosidase inhibitory activity and molecular docking studies. Bioorg. Med. Chem. 28, (21). https://doi.org/10.1016/j.bmc.2020.115605 115605.

Taha, M., Rahim, F., Uddin, N., Khan, I.U., Iqbal, N., Salahuddin, M., Zafar, A., 2021. Exploring indole-based-thiadiazole derivatives as potent acetylcholinesterase and butyrylcholinesterase enzyme inhibitors. Int. J. Biol. Macromol. 188, 1025–1036. https://doi.org/10.1016/j.ijbiomac.2021.08.065.

Thanikachalam, P.V., Maurya, R.K., Garg, V., Monga, V., 2019. An insight into the medicinal perspective of synthetic analogs of indole: A review. Eur. J. Med. Chem. 180, 562–612. https://doi.org/10.1016/j.ejmech.2019.07.019.

Turkan, F., Cetin, A., Taslimi, P., Gulçin, İ., 2018. Some pyrazoles derivatives: Potent carbonic anhydrase, α-glycosidase, and cholinesterase enzymes inhibitors. Arch. Pharm. 351 (10), 1800200. https://doi.org/10.1002/ardp.201800200.

Turkan, F., Çetin, A., Taslimi, P., Karaman, M., Gulçin, İ., 2019. Synthesis, biological evaluation and molecular docking of novel pyrazole derivatives as potent carbonic anhydrase and acetylcholinesterase inhibitors. Bioorg. Chem. 86, 420–427. https://doi.org/10.1016/j.bioorg.2019.02.013.

Türkan, F., Calimli, M.H., Kanberoğlu, G.S., Karaman, M., 2021. Inhibition effects of isoproterenol, chlorpromazine, carbamazepine, tamoxifen drugs on glutathione S-transferase, cholinesterases enzymes and molecular docking studies. J. Biomol. Struct. Dyn. 39 (9), 3277–3284. https://doi.org/10.1080/07391102.2020.1763200.

Zhan, G., Miao, R., Zhang, F., Chang, G., Zhang, L., Zhang, X., Guo, Z., 2020. Monoterpene indole alkaloids with acetylcholinesterase inhibitory activity from the leaves of Rauvolfia vomitoria. Bioorg. Chem. 102,. https://doi.org/10.1016/j.bioorg.2020.104136 104136.

Zhang, M.Z., Chen, Q., Yang, G.F., 2015. A review on recent developments of indole-containing antiviral agents. Eur. J. Med. Chem. 89, 421–441. https://doi.org/10.1016/j.ejmech.2014.10.065.